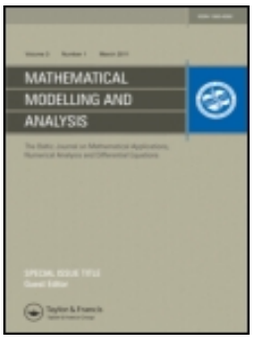

Mathematical Modelling and Analysis

ISSN: 1392-6292 (Print) 1648-3510 (Online) Journal homepage: https://www.tandfonline.com/loi/tmma20

The peridynamic equation and its spatial discretisation

E. Emmrich & O. Weckner

To cite this article: E. Emmrich & O. Weckner (2007) The peridynamic equation and its spatial discretisation, Mathematical Modelling and Analysis, 12:1, 17-27, DOI: 10.3846/1392-6292.2007.12.17-27

To link to this article: https://doi.org/10.3846/1392-6292.2007.12.17-27

Mathematical Modelling and Analysis. Ed. A.Buikis
Volume 12 Number 1, 2007, pages 17–27
 ISSN 1392-6292 print, ISSN 1648-3510 online

THE PERIDYNAMIC EQUATION AND ITS SPATIAL DISCRETISATION

E. EMMRICH[1] and O. WECKNER[2]

[1] *Technische Universität Berlin, Institut für Mathematik*

Straße des 17. Juni 136, 10623 Berlin, Germany

E-mail: emmrich@math.tu-berlin.de

[2] *Massachusetts Institute of Technology, Department of Mech. Engineering,*
Cambridge, MA 02139, USA
E-mail: olaf@weckner.de

Received November 1, 2006; revised December 15, 2006; published online February 10, 2007

Abstract. Different spatial discretisation methods for solving the peridynamic equation of motion are suggested. The methods proposed are tested for a linear microelastic material of infinite length in one spatial dimension. Moreover, the conservation of energy is studied for the continuous as well as discretised problem.

Key words: Peridynamic theory, microelastic material, integro-differential equation, numerical approximation, quadrature, energy conservation

1. Introduction

Non-local theories describing the effects of long-range interactions in elastic materials have been known for a long time, cf. [5, 6, 9] and the references cited therein. However, during the last few years, peridynamic modelling has become topical as a non-local theory in integral form that avoids any spatial differentiation, cf. [11] for a first attempt as well as e.g. [3, 4, 12, 13, 14, 15, 16]. In view of the derivative-free integral formulation, the peridynamic approach seems to be quite promising for the description of fracture, in particular of crack propagation in homogeneous and complex materials, and other problems in which discontinuities emerge such as phase transformations where the displacement gradient becomes discontinuous. For a discussion of non-local theories in solid mechanics and their application to problems of damaging, see also [1]. Other recent works on non-local theories and their application in elasticity and fracture mechanics can be found e.g. in [2, 7, 8].

The governing equation in the peridynamic theory is the second-order in time partial integro-differential equation (PIDE)

$$\rho(\boldsymbol{x})\partial_t^2\boldsymbol{u}(\boldsymbol{x},t)=\int_{\mathcal{V}}\boldsymbol{f}_{\mathrm{el}}(\boldsymbol{x},\hat{\boldsymbol{x}},\boldsymbol{u}(\boldsymbol{x},t),\boldsymbol{u}(\hat{\boldsymbol{x}},t),t)\,\mathrm{d}\hat{\boldsymbol{x}}+\boldsymbol{b}(\boldsymbol{x},t)\,, \tag{1.1}$$

in Lagrangian coordinates $\boldsymbol{x}\in\mathcal{V}$ on a time interval $(0,T)$, where ρ denotes the mass density, $\boldsymbol{u}$ the displacement field of the elastic body that occupies the volume $\mathcal{V}$, $\boldsymbol{f}_{\mathrm{el}}$ the pairwise force function that describes the internal forces, and the inhomogeneity $\boldsymbol{b}$ collects all external forces per unit volume. Equation (1.1) is supplemented by initial values for $\boldsymbol{u}(\cdot,0)$ and $\partial_t\boldsymbol{u}(\cdot,0)$. In view of the balance of the angular momentum of the mass-free bond between $\boldsymbol{x}$ and $\hat{\boldsymbol{x}}$, the pairwise force function $\boldsymbol{f}_{\mathrm{el}}$ is always in the direction of the vector pointing from the current position $\boldsymbol{x}+\boldsymbol{u}(\boldsymbol{x},t)$ to the reference position $\hat{\boldsymbol{x}}+\boldsymbol{u}(\hat{\boldsymbol{x}},t)$.

Let us suppose that the system is invariant against a rigid body motion and the internal forces are independent of time such that

$$\boldsymbol{f}_{\mathrm{el}}(\boldsymbol{x},\hat{\boldsymbol{x}},\boldsymbol{u},\hat{\boldsymbol{u}},t)=\boldsymbol{f}(\boldsymbol{x},\hat{\boldsymbol{x}},\hat{\boldsymbol{u}}-\boldsymbol{u})=-\boldsymbol{f}(\hat{\boldsymbol{x}},\boldsymbol{x},\boldsymbol{u}-\hat{\boldsymbol{u}}).$$

If the material is microelastic then there exists a pairwise potential w such that $\boldsymbol{f}(\boldsymbol{x},\hat{\boldsymbol{x}},\boldsymbol{\eta})=\nabla_{\boldsymbol{\eta}}\,w(\boldsymbol{x},\hat{\boldsymbol{x}},\boldsymbol{\eta})$. Equation (1.1) then follows from the variational problem: find

$$\boldsymbol{u}=\arg\min J(\boldsymbol{u}),\qquad J(\boldsymbol{u}):=\int_0^T\int_{\mathcal{V}}l(\boldsymbol{x},\boldsymbol{u}(\boldsymbol{x},t),t)\,\mathrm{d}\boldsymbol{x}\mathrm{d}t\,, \tag{1.2}$$

where $l=e_{\mathrm{kin}}-e_{\mathrm{el}}-e_{\mathrm{ext}}$ is the Lagrangian density and incorporates the kinetic and elastic energy densities:

$$e_{\mathrm{kin}}=\frac{1}{2}\rho(\boldsymbol{x})\,|\partial_t\boldsymbol{u}(\boldsymbol{x},t)|^2,\quad e_{\mathrm{el}}=\frac{1}{2}\int_{\mathcal{V}}w(\boldsymbol{x},\hat{\boldsymbol{x}},\boldsymbol{u}(\hat{\boldsymbol{x}},t)-\boldsymbol{u}(\boldsymbol{x},t))\,\mathrm{d}\hat{\boldsymbol{x}},$$

and the density $e_{\mathrm{ext}}=-\boldsymbol{b}(\boldsymbol{x},t)\cdot\boldsymbol{u}(\boldsymbol{x},t)$ due to the external force density $\boldsymbol{b}$.

More precisely, a solution to (1.1) also fulfills the necessary condition for being a solution to the variational problem (1.2), and a sufficiently regular solution of the necessary condition is also a solution to (1.1). It can be shown that the Gâteaux derivative $\dfrac{\mathrm{d}}{\mathrm{d}\theta}J(\boldsymbol{u}+\theta\boldsymbol{v})|_{\theta=0}$ vanishes, which is the necessary condition for a minimum, if for all $\boldsymbol{v}$ in an appropriate function space

$$\int_0^T\int_{\mathcal{V}}\rho(\boldsymbol{x})\partial_t\boldsymbol{u}(\boldsymbol{x},t)\cdot\partial_t\boldsymbol{v}(\boldsymbol{x},t)\,\mathrm{d}\boldsymbol{x}\mathrm{d}t=\frac{1}{2}\int_0^T\int_{\mathcal{V}}\int_{\mathcal{V}}\boldsymbol{f}(\boldsymbol{x},\hat{\boldsymbol{x}},\boldsymbol{u}(\hat{\boldsymbol{x}},t)-\boldsymbol{u}(\boldsymbol{x},t))\cdot$$
$$\cdot\,(\boldsymbol{v}(\hat{\boldsymbol{x}},t)-\boldsymbol{v}(\boldsymbol{x},t))\;\mathrm{d}\hat{\boldsymbol{x}}\mathrm{d}\boldsymbol{x}\mathrm{d}t-\int_0^T\int_{\mathcal{V}}\boldsymbol{b}(\boldsymbol{x},t)\cdot\boldsymbol{v}(\boldsymbol{x},t)\,\mathrm{d}\boldsymbol{x}\mathrm{d}t\,. \tag{1.3}$$

This is the space-time weak formulation of (1.1). For the second Gâteaux derivative of J at $\boldsymbol{u}$, we find

$$\int_0^T\int_{\mathcal{V}}\rho(\boldsymbol{x})\partial_t\boldsymbol{w}(\boldsymbol{x},t)\cdot\partial_t\boldsymbol{v}(\boldsymbol{x},t)\,\mathrm{d}\boldsymbol{x}\mathrm{d}t-\frac{1}{2}\int_0^T\int_{\mathcal{V}}\int_{\mathcal{V}}(\boldsymbol{w}(\hat{\boldsymbol{x}},t)-\boldsymbol{w}(\boldsymbol{x},t))\cdot$$
$$\cdot\nabla_{\boldsymbol{\eta}}\,\boldsymbol{f}(\boldsymbol{x},\hat{\boldsymbol{x}},\boldsymbol{u}(\hat{\boldsymbol{x}},t)-\boldsymbol{u}(\boldsymbol{x},t))\cdot(\boldsymbol{v}(\hat{\boldsymbol{x}},t)-\boldsymbol{v}(\boldsymbol{x},t))\;\mathrm{d}\hat{\boldsymbol{x}}\mathrm{d}\boldsymbol{x}\mathrm{d}t\,.$$

This shows that the functional J is strictly convex if for all $\boldsymbol{x}, \hat{\boldsymbol{x}}$ and $\boldsymbol{\eta} \neq 0$

$$\boldsymbol{\eta} \cdot \nabla_{\boldsymbol{\eta}} \boldsymbol{f}(\boldsymbol{x}, \hat{\boldsymbol{x}}, \boldsymbol{\eta}) \cdot \boldsymbol{\eta} = \boldsymbol{\eta} \cdot \nabla^2_{\boldsymbol{\eta}} w(\boldsymbol{x}, \hat{\boldsymbol{x}}, \boldsymbol{\eta}) \cdot \boldsymbol{\eta} > 0$$

holds true, which e.g. justifies also the linear ansatz

$$\boldsymbol{f}(\boldsymbol{x}, \hat{\boldsymbol{x}}, \boldsymbol{\eta}) = \boldsymbol{f_0}(\boldsymbol{x}, \hat{\boldsymbol{x}}) + \boldsymbol{C}(\boldsymbol{x}, \hat{\boldsymbol{x}}) \cdot \boldsymbol{\eta} \tag{1.4}$$

with a positive definite stiffness tensor $\boldsymbol{C} = \boldsymbol{C}(\boldsymbol{x}, \hat{\boldsymbol{x}})$ and $\boldsymbol{f_0}$ denoting forces in the reference configuration (prestressed configuration) that will be assumed to be zero in what follows. For a stiffness tensor $\boldsymbol{C}$ that is assumed to be symmetric with respect to its arguments and its tensor structure,

$$\boldsymbol{C}(\hat{\boldsymbol{x}}, \boldsymbol{x}) = \boldsymbol{C}(\boldsymbol{x}, \hat{\boldsymbol{x}}), \quad \boldsymbol{C}(\boldsymbol{x}, \hat{\boldsymbol{x}})^{\mathsf{T}} = \boldsymbol{C}(\boldsymbol{x}, \hat{\boldsymbol{x}}), \tag{1.5}$$

but needs not to be of convolution type or definite, the corresponding potential is given by $w(\boldsymbol{x}, \hat{\boldsymbol{x}}, \boldsymbol{\eta}) = \boldsymbol{\eta} \cdot \boldsymbol{C}(\boldsymbol{x}, \hat{\boldsymbol{x}}) \cdot \boldsymbol{\eta}/2$. Equation (1.1) then reads as

$$\rho(\boldsymbol{x}) \partial_t^2 \boldsymbol{u}(\boldsymbol{x}, t) = \int_{\mathcal{V}} \boldsymbol{C}(\boldsymbol{x}, \hat{\boldsymbol{x}}) \cdot (\boldsymbol{u}(\hat{\boldsymbol{x}}, t) - \boldsymbol{u}(\boldsymbol{x}, t)) \, \mathrm{d}\hat{\boldsymbol{x}} + \boldsymbol{b}(\boldsymbol{x}, t). \tag{1.6}$$

Regarding the conservation of the total energy, we can prove the following theorem by employing the usual energy method.

Theorem 1. *Let $\boldsymbol{u}$ be a sufficiently smooth displacement field and let the pairwise force function be given by* (1.4) *with a stiffness tensor that fulfills* (1.5). *The total energy remains constant if the external forces are autonomous,*

$$\frac{\mathrm{d}}{\mathrm{d}t}\big(\mathcal{E}_{\mathrm{kin}}(t) + \mathcal{E}_{\mathrm{el}}(t) + \mathcal{E}_{\mathrm{ext}}(t)\big) = 0,$$

where $\mathcal{E}_i(t) = \int_{\mathcal{V}} e_i(\boldsymbol{x}, \boldsymbol{u}(\boldsymbol{x}, t), t) \, \mathrm{d}\boldsymbol{x}$ ($i \in \{\mathrm{kin}, \mathrm{el}, \mathrm{ext}\}$). Otherwise, there holds for all $t \in (0, T)$ and $\nu > 0$

$$\begin{aligned} &\mathcal{E}_{\mathrm{kin}}(t) + \mathcal{E}_{\mathrm{el}}(t) + \nu \int_0^t \mathrm{e}^{\nu(t-s)} \mathcal{E}_{\mathrm{el}}(s) \, \mathrm{d}s \\ &\qquad \leq \mathrm{e}^{\nu t} \left(\mathcal{E}_{\mathrm{kin}}(0) + \mathcal{E}_{\mathrm{el}}(0)\right) + \frac{1}{2\nu} \int_0^t \int_{\mathcal{V}} \frac{\mathrm{e}^{\nu(t-s)}}{\rho(\boldsymbol{x})} |\boldsymbol{b}(\boldsymbol{x}, t)|^2 \, \mathrm{d}\boldsymbol{x}\mathrm{d}s. \end{aligned}$$

A similar result can also be found in [11] for microelastic media.

Numerical studies so far rely upon the meshfree Emu code (cf. [10]) that solves (1.1) by a quadrature formula method on a (not necessarily) equidistant grid with the composite midpoint rule. The resulting ODE system is solved using a central difference approximation of the time derivative. The midpoint rule is one of the methods considered in this paper. Another approach based upon the Gauß-Hermite quadrature and the composite trapezoidal rule has been suggested by the authors in [4, 16] for an infinite bar. As is shown in [4], the peridynamic modelling is also advantageous from the numerical point of view since initial jump discontinuities either in the displacement or the velocity field remain for all times at the same Lagrangian location, cf. also

[15]. This can be used in the numerical approximation for a sharp resolution of the discontinuities.

In this paper, three different discretisation methods –based upon the Gauß-Hermite (GH) quadrature, the composite midpoint (MP) rule, and linear finite elements (FE)– are presented for the unbounded one-dimensional case $\mathcal{V} = \mathbb{R}$. All these methods can quite easily be extended to meshfree approximations for the two- or three-dimensional case. Whereas the Gauß-Hermite quadrature with its non-equidistant quadrature points is especially suited for an unbounded spatial domain, we employ the composite midpoint rule and the finite element method with an equidistant partition that avoids additional computational costs.

Specialised to an infinite one-dimensional, linear, and pairwise equilibrated body, the equation of motion (1.1) reads for $(x,t) \in \mathbb{R} \times (0,T)$ as

$$\rho(x)\partial_t^2 u(x,t) = \int_{-\infty}^{+\infty} C(x,\hat{x})\,(u(\hat{x},t) - u(x,t))\,\mathrm{d}\hat{x} + b(x,t)\,. \tag{1.7}$$

Here, C with $C(\hat{x},x) = C(x,\hat{x})$ is the stiffness distribution density or so-called micromodulus function. The initial-value problem for this PIDE has been analysed in detail by the authors in [4], where existence, uniqueness, and stability have been proven in the space of functions that are Bochner integrable with respect to time and essentially bounded with respect to space. We test the methods suggested for an initial-value problem for (1.7) with a micromodulus function $C(x,\hat{x}) \sim \ell^{-3}\mathrm{e}^{-\ell^{-2}(\hat{x}-x)^2}$ (ℓ is a length-scale parameter), a Gaußian distribution for the initial displacement, and zero initial velocity. Although ℓ characterises the peridynamic horizon, which is the radius of the neighbourhood in which material particles are assumed to interact with each other, we are dealing here with an infinite horizon as $C(x,\hat{x}) \neq 0$ for all $x,\hat{x} \in \mathbb{R}$.

2. Spatial Approximation

The *Gauß-Hermite* quadrature reads as

$$\int_{-\infty}^{\infty} \mathrm{e}^{-x^2}\Phi(x)\mathrm{d}x \approx \sum_{j=0}^{N} \sigma_j^{\mathrm{GH}}\Phi(x_j^{\mathrm{GH}})$$

for given $N \in \mathbb{N}$ with the roots x_j^{GH} $(j = 0,1,\ldots,N)$ of the Hermite polynomial $H_{N+1}(x)$ and the quadrature weights σ_j^{GH}

$$H_{N+1}(x) := (-1)^{N+1}\mathrm{e}^{x^2}\frac{\mathrm{d}^{N+1}\mathrm{e}^{-x^2}}{\mathrm{d}x^{N+1}}, \quad \sigma_j^{\mathrm{GH}} = 2^{N+2}\,(N+1)!\frac{\sqrt{\pi}}{H_{N+2}(x_j^{\mathrm{GH}})^2}.$$

The Gauß-Hermite quadrature is exact for polynomials $\Phi = \Phi(x)$ of highest degree $2N+1$.

Applying the quadrature formula method with the Gauß-Hermite quadrature to (1.7) leads to the coupled ODE system $(i = 0,1,\ldots,N\,,\ t \in (0,T))$

$$\rho(x_i^{\mathrm{GH}})\ddot{u}_i^{\mathrm{GH}}(t) = \sum_{j=0}^{N} \sigma_j^{\mathrm{GH}} \mathrm{e}^{\left(x_j^{\mathrm{GH}}\right)^2} C(x_i^{\mathrm{GH}}, x_j^{\mathrm{GH}}) \left(u_j^{\mathrm{GH}}(t) - u_i^{\mathrm{GH}}(t)\right) + b(x_i^{\mathrm{GH}}, t)\,, \quad (2.1)$$

where $u_i^{\mathrm{GH}}(t)$ is an approximation for $u(x_i^{\mathrm{GH}}, t)$. As usual, the (double) dot denotes the (second) time derivative. The system is supplemented by the (pointwise restriction of the) initial values $u(\cdot, 0)$ and $\partial_t u(\cdot, 0)$. Multiplying (2.1) by $\sigma_i^{\mathrm{GH}} \mathrm{e}^{\left(x_i^{\mathrm{GH}}\right)^2}$ and with $b_i^{\mathrm{GH}}(t) = \sigma_i^{\mathrm{GH}} \mathrm{e}^{\left(x_i^{\mathrm{GH}}\right)^2} b(x_i^{\mathrm{GH}}, t)$ and

$$\begin{aligned} M_{ij}^{\mathrm{GH}} &:= \sigma_i^{\mathrm{GH}} \mathrm{e}^{\left(x_i^{\mathrm{GH}}\right)^2} \rho(x_i^{\mathrm{GH}}) \delta_{ij}\,, \\ K_{ij}^{\mathrm{GH}} &= \sum_{k=0}^{N} \sigma_i^{\mathrm{GH}} \mathrm{e}^{\left(x_i^{\mathrm{GH}}\right)^2} \sigma_k^{\mathrm{GH}} \mathrm{e}^{\left(x_k^{\mathrm{GH}}\right)^2} C(x_i^{\mathrm{GH}}, x_k^{\mathrm{GH}})\, \delta_{ij} \\ &\quad - \sigma_i^{\mathrm{GH}} \mathrm{e}^{\left(x_i^{\mathrm{GH}}\right)^2} \sigma_j^{\mathrm{GH}} \mathrm{e}^{\left(x_j^{\mathrm{GH}}\right)^2} C(x_i^{\mathrm{GH}}, x_j^{\mathrm{GH}}), \end{aligned}$$

we may rewrite the system (2.1) as

$$M^{\mathrm{GH}} \ddot{u}^{\mathrm{GH}}(t) + K^{\mathrm{GH}} u^{\mathrm{GH}}(t) = b^{\mathrm{GH}}(t)\,, \quad t \in (0, T)\,. \quad (2.2)$$

Due to the scaling of (2.1), the mass as well as stiffness matrix is symmetric.

Based upon the underlying quadrature, we may compute approximations for the kinetic, elastic, and external energy:

$$\begin{aligned} \mathcal{E}_{\mathrm{kin}}^{\mathrm{GH}}(t) &= \frac{1}{2} \sum_{i=0}^{N} \sigma_i^{\mathrm{GH}} \mathrm{e}^{\left(x_i^{\mathrm{GH}}\right)^2} \rho(x_i^{\mathrm{GH}}) \dot{u}_i^{\mathrm{GH}}(t)^2 = \frac{1}{2} \dot{u}^{\mathrm{GH}}(t)^{\mathsf{T}} M^{\mathrm{GH}} \dot{u}^{\mathrm{GH}}(t)\,, \\ \mathcal{E}_{\mathrm{el}}^{\mathrm{GH}}(t) &= \frac{1}{4} \sum_{i,j=0}^{N} \sigma_i^{\mathrm{GH}} \mathrm{e}^{\left(x_i^{\mathrm{GH}}\right)^2} \sigma_j^{\mathrm{GH}} \mathrm{e}^{\left(x_j^{\mathrm{GH}}\right)^2} C(x_i^{\mathrm{GH}}, x_j^{\mathrm{GH}}) \left(u_j^{\mathrm{GH}}(t) - u_i^{\mathrm{GH}}(t)\right)^2 \\ &= \frac{1}{2} u^{\mathrm{GH}}(t)^{\mathsf{T}} K^{\mathrm{GH}} u^{\mathrm{GH}}(t)\,, \\ \mathcal{E}_{\mathrm{ext}}^{\mathrm{GH}}(t) &= -\sum_{i=0}^{N} \sigma_i^{\mathrm{GH}} \mathrm{e}^{\left(x_i^{\mathrm{GH}}\right)^2} b(x_i^{\mathrm{GH}}, t)\, u_i^{\mathrm{GH}}(t) = -u^{\mathrm{GH}}(t)^{\mathsf{T}} b^{\mathrm{GH}}(t)\,. \end{aligned} \quad (2.3)$$

For the *composite midpoint rule*, which forms the basis of the Emu code (cf. [10]), we observe the following. Let N be an even integer, $h > 0$, and $x_j^{\mathrm{MR}} = (j - N/2)h$ $(j = 0, 1, \ldots, N)$. The internal force at point x is then approximated on the numerical domain $[-(N+1)h/2, (N+1)h/2]$ by

$$\begin{aligned} \int_{-\infty}^{\infty} C(x, \hat{x}) \left(u(\hat{x}, t) - u(x, t)\right) \mathrm{d}\hat{x} &\approx \sum_{j=0}^{N} \int_{x_j^{\mathrm{MR}} - \frac{h}{2}}^{x_j^{\mathrm{MR}} + \frac{h}{2}} C(x, \hat{x}) \left(u(\hat{x}, t) - u(x, t)\right) \mathrm{d}\hat{x} \\ &\approx h \sum_{j=0}^{N} C(x, x_j^{\mathrm{MR}}) \left(u(x_j^{\mathrm{MR}}, t) - u(x, t)\right)\,. \end{aligned}$$

This leads again to a system of the type (2.2) with $b_i^{\mathrm{MR}}(t) = hb(x_i^{\mathrm{MR}}, t)$ and

$$M_{ij}^{\mathrm{MR}} = h\,\rho(x_i^{\mathrm{MR}})\delta_{ij}\,,\ K_{ij}^{\mathrm{MR}} = h^2 \sum_{k=0}^{N} C(x_i^{\mathrm{MR}}, x_k^{\mathrm{MR}})\,\delta_{ij} - C(x_i^{\mathrm{MR}}, x_j^{\mathrm{MR}})\,.$$

The discrete energies are given analogously to (2.3).

The numerical scheme relying upon *linear finite elements* is derived from the spatial weak formulation

$$\int_{-\infty}^{\infty} \rho(x)\partial_t^2 u(x,t)v(x)\,\mathrm{d}x + \frac{1}{2}\int_{-\infty}^{\infty}\int_{-\infty}^{\infty} (u(\hat{x},t) - u(x,t)) \times C(x,\hat{x})\,(v(\hat{x}) - v(x))\,\mathrm{d}\hat{x}\,\mathrm{d}x = \int_{-\infty}^{\infty} b(x,t)\,v(x)\,\mathrm{d}x \quad (2.4)$$

for all v in an appropriate function space. Let $N \in \mathbb{N}$ be even and $h > 0$. Moreover, let g_i $(i = 0, 1, \ldots, N)$ be the linear hat functions with respect to the equidistant nodes $x_j^{\mathrm{FE}} = x_j^{\mathrm{MR}} = (j - N/2)h$ $(j = 0, 1, \ldots, N)$ such that, in particular, $g_i(x_j^{\mathrm{FE}}) = \delta_{ij}$. Outside the numerical domain $[-Nh/2 - h, Nh/2 + h]$, we extend the hat functions g_i by zero. Substituting the Ritz-Galerkin ansatz

$$u_N(x,t) = \sum_{j=0}^{N} u_j^{\mathrm{FE}}(t) g_j(x)$$

into the weak formulation above and testing with g_i, we again come up with a system of the type (2.2) with

$$b_i^{\mathrm{FE}}(t) = \int_{-\infty}^{\infty} b(x,t)g_i(x)\,\mathrm{d}x\,,\ M_{ij}^{\mathrm{FE}} = \int_{-\infty}^{\infty} \rho(x)g_i(x)g_j(x)\,\mathrm{d}x\,,$$
$$K_{ij}^{\mathrm{FE}} = \frac{1}{2}\int_{-\infty}^{\infty}\int_{-\infty}^{\infty} (g_j(\hat{x}) - g_j(x))\,C(x,\hat{x})\,(g_i(\hat{x}) - g_i(x))\,\mathrm{d}\hat{x}\mathrm{d}x\,.$$

Again, $u_i^{\mathrm{FE}}(t) = u_N(x_i^{\mathrm{FE}}, t)$ is an approximation for $u(x_i^{\mathrm{FE}}, t)$. The mass matrix M^{FE} as well as the stiffness matrix K^{FE} is symmetric. Moreover, the integrals appearing are proper and the mass matrix is tridiagonal due to the compact support of the basis functions. The stiffness matrix is, however, not sparse in view of the infinite horizon. Nevertheless, the matrix entries decrease with increasing distance from the diagonal. A possible variation of this method might be a mass lumping. For the discrete energies, we find, from replacing u by u_N in the definition of the energies, that again (2.3) holds true (replacing GH by FE).

Remark 1. In the continuous problem, a rigid translation of all particles corresponding to an arbitrary choice of the origin causes no deformation and, therefore, no internal force acting on any particle x. The same applies to the discrete problem arising from the Gauß-Hermite or composite midpoint quadrature since the row sums in the stiffness matrices vanish. For the FE

discretisation as described above, the row sums are only approximately zero. Choosing only half hats for the first and last shape function, the row sums become exactly zero. Interpreting the numerical scheme as a discretisation of an originally finite system, it remains open to investigate which kind of boundary effects corresponds to this choice of shape functions.

It is an easy task to show that any quadrature formula method applied to the PIDE (1.7) satisfies the energy equation in the discrete sense and conserves the discrete total energy for autonomous external forces if the discrete energies are defined appropriately as is e.g. conducted above for the Gauß-Hermite quadrature. The same applies to any Galerkin method.

3. Test Problem and Numerical Results

In order to test and compare the numerical methods suggested, we consider (1.7) with the micromodulus function

$$C(x,\hat{x}) = 4E\mathrm{e}^{-(\hat{x}-x)^2/\ell^2}/(\ell^3\sqrt{\pi})$$

and the initial conditions and right-hand side

$$u(x,0) = u_0(x) = U\mathrm{e}^{-x^2/L^2},\quad \partial_t u(x,0) = v_0(x) \equiv 0,\quad b(x,t) \equiv 0.$$

Here, E denotes the Young modulus, $\ell > 0$ a length-scale parameter, which models the non-locality and is discussed in detail in [15], $L > 0$ another length-scale parameter, which describes the initial displacement, and U the maximal initial displacement. As we assume a homogeneous material, we also have $\rho(x) \equiv \rho_0$. The exact solution is given by

$$u(x,t;\ell) = \frac{2U}{\sqrt{\pi}}\int_0^\infty \mathrm{e}^{-\omega^2}\cos\left(\frac{2\omega x}{L}\right)\cos\left(\frac{2c_0 t}{\ell}\sqrt{1-\mathrm{e}^{-\omega^2\ell^2/L^2}}\right)\mathrm{d}\omega\,, \quad (3.1)$$

where $c_0 = \sqrt{E/\rho_0}$ is the velocity of sound (cf. [15]), and can be used to estimate the discretisation error. In the limit $\ell \to 0$, the peridynamic equation becomes the classical wave equation of local elasticity theory and the peridynamic solution converges indeed towards the d'Alembert solution.

The numerical results are presented for the normalised quantities

$$\zeta = \frac{x}{L},\quad \tau = \frac{c_0 t}{L},\quad \eta(\zeta,\tau) = \frac{u(x,t)}{U},\quad \lambda = \frac{\ell}{L},$$

$$\tilde{\mathcal{E}}_{\mathrm{kin}}(t) = \frac{L\mathcal{E}_{\mathrm{kin}}(t)}{EU^2},\quad \tilde{\mathcal{E}}_{\mathrm{el}}(t) = \frac{L\mathcal{E}_{\mathrm{el}}(t)}{EU^2}.$$

Moreover, we choose $\lambda = 0.75$ in order to have a significant influence of the non-locality. In view of the initial conditions, it follows

$$\tilde{\mathcal{E}}_{\mathrm{kin}}(t) + \tilde{\mathcal{E}}_{\mathrm{el}}(t) = \tilde{\mathcal{E}}_{\mathrm{kin}}(0) + \tilde{\mathcal{E}}_{\mathrm{el}}(0) = \frac{\sqrt{\pi}}{2\sqrt{2}}f(\lambda),\quad f(\lambda) := \frac{4}{\lambda^2}\Big(1 - \frac{\sqrt{2}}{\sqrt{2+\lambda^2}}\Big).$$

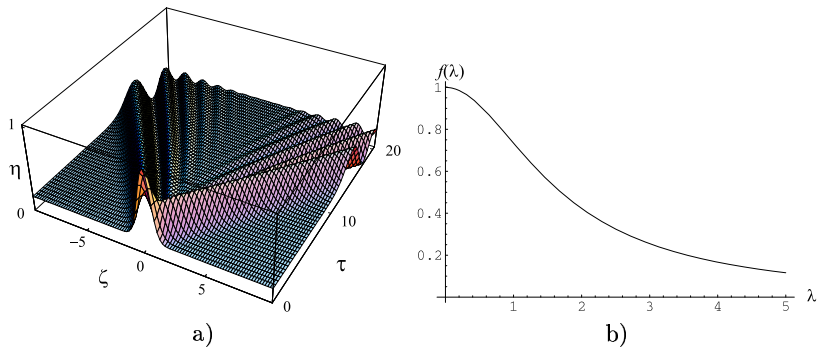

Figure 1. Numerical solutions: a) peridynamic solution, b) function $f = f(\lambda)$.

Note that $\lim_{\lambda\to 0} f(\lambda) = 1$, whereas $\lim_{\lambda\to\infty} f(\lambda) = 0$. In particular, we obtain in the limit $\lambda \to 0$ the classical strain energy

$$\mathcal{E}_{\mathrm{el}}(0) = \frac{E}{2}\int_{-\infty}^{\infty} u_0'(x)^2 \,\mathrm{d}x = EU^2\sqrt{\pi}/(2\sqrt{2}\,L)$$

of a bar in linear elasticity theory with the initial displacement u_0 as above. Therefore, $f = f(\lambda)$ describes the ratio of the elastic energy in the non-local peridynamic model and the classical strain energy. As is seen in Fig. 1, the more non-local the material is, the less elastic energy is stored in it. Note again that the initial elastic energy equals the total energy. It might be interesting to study whether this comparison still holds true in general, i.e. whether a non-local material always possesses a lower *total* energy as a classical material when the initial conditions remain the same.

In order to compare the numerical results for given N, the spatial grid size h is taken such that for all methods the numerical domain is the same as determined by the Gauß-Hermite quadrature. Therefore, the numerical domain becomes larger with an increasing number of quadrature points. It should be noted that in the case of finite elements, the integrals appearing are simplified as far as possible but the remaining Gaußian integrals are calculated numerically using Mathematica. Moreover, our numerical computations rely upon the exact solution of the corresponding ODE system. The numerical results are compared with the normalised exact solution given by (3.1). In order to calculate the integral in (3.1), we again use Mathematica.

Fig. 2 shows the interpolated numerical solution for different numbers of quadrature points. As one can infer from Fig. 2, there are artificial wave reflections at the boundaries of the numerical domain after some time. These reflections appear the later, the greater the spatial domain of computation is.

Moreover, these reflections seem to cause oscillations in the kinetic and elastic energy as is shown in Fig. 3. Similar results are obtained for the other methods. The conservation of the total energy is exactly reproduced by all methods as is expected.

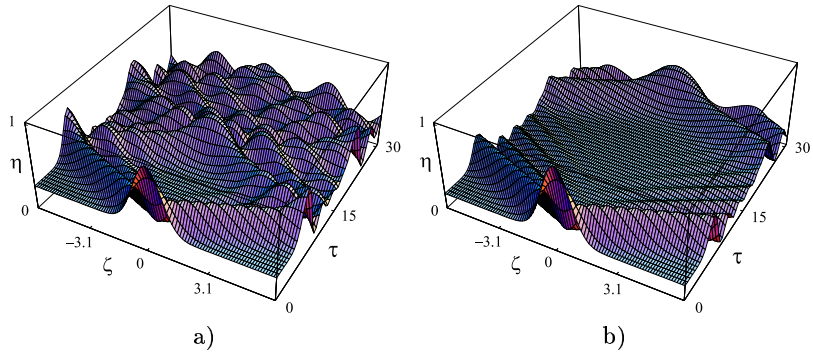

Figure 2. Numerical solution GH with different parameters: a) $N = 24$, b) $N = 98$.

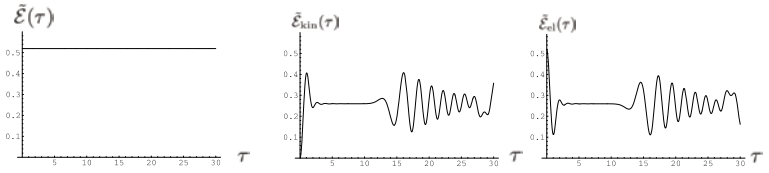

Figure 3. Discrete energies (GH with $N = 98$): a) total, b) kinetic, c) elastic energy
.

In Fig. 4, the displacement of the origin is presented. The plotted numerical solution coincides with the exact solution up to some time when the spurious wave reflections deteriorate the numerical solution. Similar results are again obtained for the other methods.

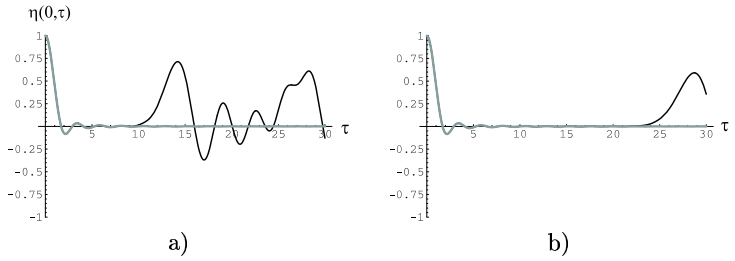

Figure 4. Exact (grey) and numerical (black) displacement of the origin GH with a) $N = 24$, b) $N = 98$.

What follows in Figs. 5, 6, and 7 is the error between the exact and the numerical solution, measured in the L^2-norm over the numerical domain, for the different methods.

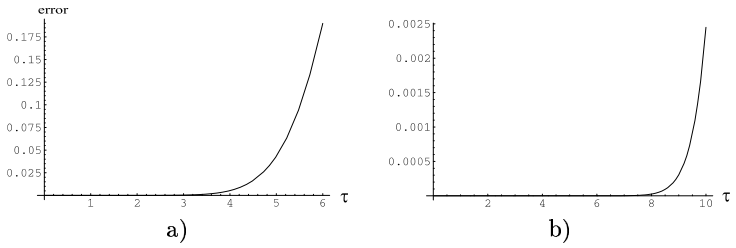

Figure 5. Error as a function of time for GH with a) $N = 24$, b) $N = 98$.

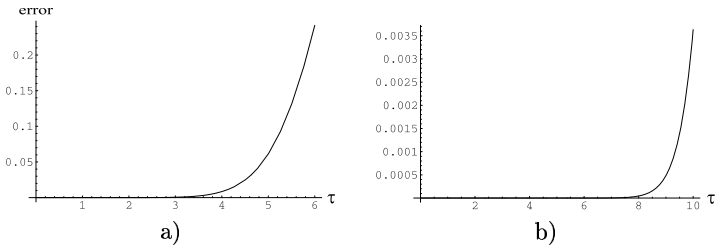

Figure 6. Error as a function of time for MP with a) $N = 24$, b) $N = 98$.

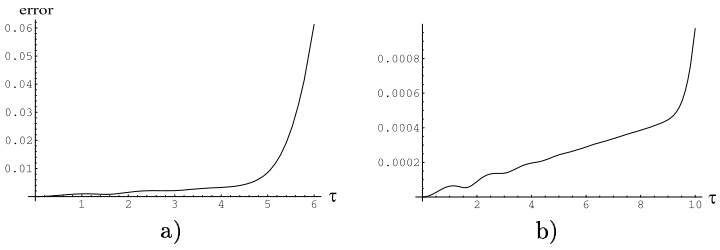

Figure 7. Error as a function of time for FE with a) $N = 24$, b) $N = 98$.

It turns out that the Gauß-Hermite quadrature and the composite midpoint rule give almost the same accuracy, GH being somewhat better. The Gauß-Hermite quadrature, which is particularly suitable for an unbounded domain as in our test problem, requires, however, the rather costly computation of the roots of the Hermite polynomials. With the finite element method,

the best accuracy is achieved. However, in view of the definition of the stiffness matrix, which is not sparse, the finite element method requires more computations than the quadrature formula method.

References

[1] Z. P. Bažant and M. Jirásek. Nonlocal integral formulations of plasticity and damage: survey and progress. *J. Eng. Mech.*, **128**(11), 1119–1149, 2002.

[2] Y. Chen, J. D.Lee and A. Eskandarian. Dynamic meshless method applied to nonlocal crack problems. *Theor. Appl. Fract. Mech.*, **38**, 293–300, 2002.

[3] K. Dayal and K. Bhattacharya. Kinetics of phase transformations in the peridynamic formulation of continuum mechanics. *J. Mech. Phys. Solids*, **54**(9), 1811–1842, 2006.

[4] E. Emmrich and O. Weckner. Analysis and numerical approximation of an integro-differential equation modelling non-local effects in linear elasticity. *Math. Mech. Solids*, 2005.

[5] A. C. Eringen. Vistas of nonlocal continuum physics. *Int. J. Eng. Sci.*, **30**(10), 1551–1565, 1992.

[6] I. A. Kunin. *Elastic Media with Microstructure.* Springer, Berlin, 1982/83.

[7] A. A. Pisano and P. Fuschi. Closed form solution for a nonlocal elastic bar in tension. *Int. J. Solids Structures*, **40**(1), 13–23, 2003.

[8] C. Polizzotto. Nonlocal elasticity and related variational principles. *Int. J. Solids Structures*, **38**, 42–43, 7359–7380, 2001.

[9] D. Rogula. *Nonlocal Theory of Material Media.* Springer, Berlin, 1982.

[10] S. A. Silling. *About Emu.* http://www.sandia.gov/emu/emu.htm.

[11] S. A. Silling. Reformulation of elastic theory for discontinuities and long-range forces. *J. Mech. Phys. Solids*, **48**(1), 175–209, 2000.

[12] S. A. Silling and E. Askari. A meshfree method based on the peridynamic model of solid mechanics. *Computers & Structures*, **83**, 1526–1535, 2005.

[13] S. A. Silling and F. Bobaru. Peridynamic modeling of membranes and fibers. *Int. J. Non-linear Mech.*, **40**, 395–409, 2005.

[14] S. A. Silling, M. Zimmermann and R. Abeyaratne. Deformation of a peridynamic bar. *J. Elasticity*, **73**, 173–190, 2003.

[15] O. Weckner and R. Abeyaratne. The effect of long-range forces on the dynamics of a bar. *J. Mech. Phys. Solids*, **53**(3), 705–728, 2005.

[16] O. Weckner and E. Emmrich. Numerical simulation of the dynamics of a nonlocal, inhomogeneous, infinite bar. *JCAM*, **6**(2), 311–319, 2005.